

**Recycling carbon dioxide in the cement industry to produce added-value additives: a step towards a CO<sub>2</sub> circular economy**

# **Deliverable D7.4**

## **Report on the assessment of the quality increase of cements enabled by the RECODE CO<sub>2</sub>-derived additives**

WP7 – Evaluation of product quality as cement additives

Version Draft

**Authors:** Isabella Cosentino (POLITO), Giuseppe Andrea Ferro (POLITO), Luciana Restuccia (POLITO)

**Lead participant:** POLITO

**Delivery date:** 31 July 2021


**Dissemination level:** Public

**Type:** Report




*This project has received funding from the European Union's Horizon 2020 Research and Innovation Programme under Grant Agreement No. 768583. The content of this publication is the sole responsibility of the authors. The European Commission or its services cannot be held responsible for any use that may be made of the information it contains.*



	<b>Title</b> <b>Report on the assessment of the quality increase of cements enabled by the RECODE CO<sub>2</sub>-derived additives</b>	<b>Deliverable number</b> <b>D7.5</b>
		<b>Version</b> <b>Final</b>


## Revision History

<b>Author Name, Partner short name</b>	<b>Description</b>	<b>Date</b>
Isabella Cosentino (POLITO), Giuseppe Andrea Ferro (POLITO), Luciana Restuccia (POLITO)	Draft deliverable	16/07/2021
(TITAN)	Revision 1	23/07/2021
Isabella Cosentino (POLITO), Giuseppe Andrea Ferro (POLITO), Luciana Restuccia (POLITO)	Final version	31/07/2021

	<b>Title</b> <b>Report on the assessment of the quality increase of cements enabled by the RECODE CO<sub>2</sub>-derived additives</b>	<b>Deliverable number</b> <b>D7.5</b>
		<b>Version</b> <b>Final</b>

## Table of Contents

<b>Revision History .....</b>	<b>2</b>
<b>Table of Contents.....</b>	<b>3</b>
<b>1 Introduction .....</b>	<b>4</b>
<b>2 CaCO<sub>3</sub> as nanofiller in cement .....</b>	<b>4</b>
<b>3 Performance of CaCO<sub>3</sub> in cement mortars .....</b>	<b>6</b>
3.1 Characterization of the commercial CaCO <sub>3</sub> .....	6
3.2 Preparation of cement mortars .....	7
3.3 Mechanical test activity .....	8
3.4 CaCO <sub>3</sub> particles synthesized using the PBR.....	14
<b>4 Performance of CaCO<sub>3</sub> in concrete.....</b>	<b>15</b>
4.1 Materials and methods.....	15
4.2 Results and discussion .....	23
<b>5 Conclusions .....</b>	<b>28</b>
<b>References.....</b>	<b>29</b>

	<b>Title</b> <b>Report on the assessment of the quality increase of cements enabled by the RECODE CO<sub>2</sub>-derived additives</b>	<b>Deliverable number</b> <b>D7.5</b>
		<b>Version</b> <b>Final</b>

## 1 Introduction

This deliverable reports the assessment of the quality increase of cements enabled by the RECODE CO<sub>2</sub>-derived additives.


Synthesized CaCO<sub>3</sub> from CO<sub>2</sub> through the carbonation route was employed to improve mechanical properties of cementitious materials due to their physical effect such as filling voids and the nucleation effect as well as their chemical reactive. Firstly, the cement content was partially replaced with CaCO<sub>3</sub> nanoparticles. Secondly, CaCO<sub>3</sub> was added to the cement matrix. The effect of the three polymorphic forms of CaCO<sub>3</sub> (calcite, vaterite and aragonite) on the mechanical properties of cement mortars was also investigated. The production of CaCO<sub>3</sub> through carbonation is a very promising solution to mitigate CO<sub>2</sub> emissions. The application of this approach in the cement industry could allow the development of a circular economy that exploits the CO<sub>2</sub> generated in the cement manufacturing process. This circular economy approach could represent 69% of the emissions saving of the cement industry. [1]

## 2 CaCO<sub>3</sub> as nanofiller in cement

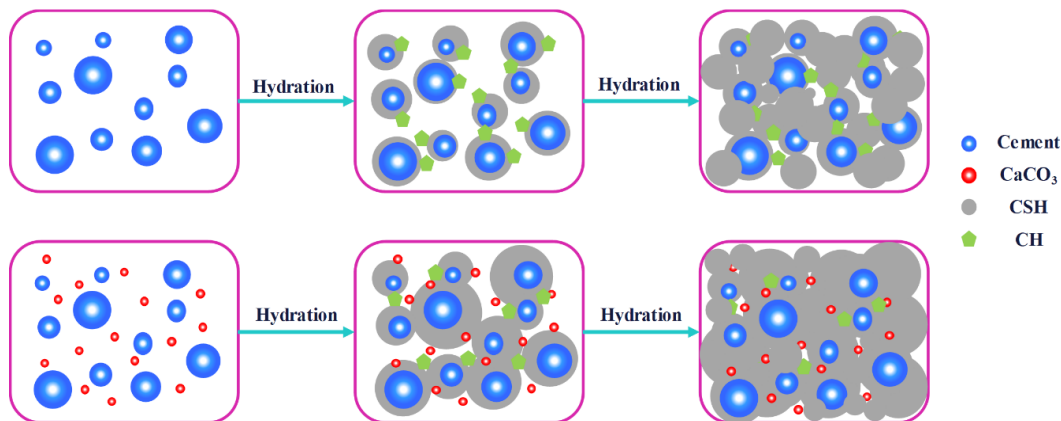
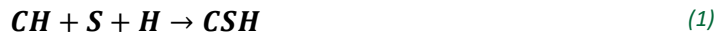


*Figure 1. Effect of nano CaCO<sub>3</sub> nanofiller on cement hydration*

CaCO<sub>3</sub> has a partly chemical and partly physical effect when used as nanofiller in cementitious materials, as illustrated in Figure 1. The particle distribution size and morphology provide a suitable environment to accelerate cement hydration. Furthermore, these properties make it possible to fill the nano and micro-voids of the cement paste structure. Thus, they decrease cement matrix porosity and hinder crack propagation [2]. This dual effect has a synergistic influence on improving the strength and durability of the cementitious materials [3]. The acceleration of hydration is caused by the chemical interaction between CaCO<sub>3</sub> and clinker. Much research reveals that nanoparticles act as a nucleation site in cement hydration, thus accelerating the hydration rate [4]–[7]. Cement hydration occurs when anhydrous cement or one of its constituent phases is mixed with water [8]. Tricalcium silicate (C<sub>3</sub>S), dicalcium silicate (C<sub>2</sub>S), tricalcium aluminate (C<sub>3</sub>A) and tetra calcium aluminoferrite (C<sub>4</sub>AF) react following the mechanism represented in Figure 2. The hydration of C<sub>3</sub>S and C<sub>2</sub>S produces calcium hydroxide (CH) and amorphous calcium silicate hydrate (CSH), which provide strength to cementitious materials [8], [9]. The hydration of

	<b>Title</b> <b>Report on the assessment of the quality increase of cements enabled by the RECODE CO<sub>2</sub>-derived additives</b>	<b>Deliverable number</b> <b>D7.5</b>
		<b>Version</b> <b>Final</b>

C<sub>3</sub>A produces calcium aluminate hydrate (CAH), while CH/C<sub>4</sub>AF hydration forms tetra calcium alumino-13-hydrate (C<sub>4</sub>AH<sub>13</sub>) and tetra calcium ferrite-13-hydrate (C<sub>4</sub>FH<sub>13</sub>). In blended cement, the generated CH reacts with active silica and alumina in the presence of water to make further CSH and calcium aluminate hydrate (CAH) during the pozzolanic reaction as follows (eq.(1) and (2):



The water/cement ratio or the composition of the cement and aggregates can influence the transformation of anhydrous compounds into the corresponding hydrates. Atmospheric conditions are also important in this process. CO<sub>2</sub> could react with the resulting CSH in the formation of CaCO<sub>3</sub> and anhydrous silica, which would reduce the strength of the cement composites. Hence, high humidity and an atmosphere with free CO<sub>2</sub> are favourable conditions for the process [8].

The CaCO<sub>3</sub> performance in cementitious materials depends on several factors, including the CaCO<sub>3</sub> content. Much research focuses on 1-3% of CaCO<sub>3</sub> content in different cementitious materials [2], [6], [7], [10]–[12]. Liu et al. [10], [11] obtained the best performance in terms of flexural and compressive strength by employing 1% of nano CaCO<sub>3</sub> in cement paste. Moreover, they found that by increasing the CaCO<sub>3</sub> content (2% and 3%), there was only an improvement in the hydration, i.e. in the early stage of the cement curing. Similarly, Supit et al. [6], [7] and Sun et al. [12] also obtained better results with 1% of CaCO<sub>3</sub> in high volume fly ash mortars and concretes. Hakamy [2] also studied fracture toughness, and the best performance was obtained with 1% of CaCO<sub>3</sub>. The increase of the CaCO<sub>3</sub> content over 1% reduced the performance of cementitious materials due to inadequate dispersion and agglomeration of nanoparticles, which affect the interaction between the nanoparticles and the cement matrix [2], [10]. In addition, the denser matrix due to the addition of nano CaCO<sub>3</sub> could be not able to provide available space for the formation of the hydration products.

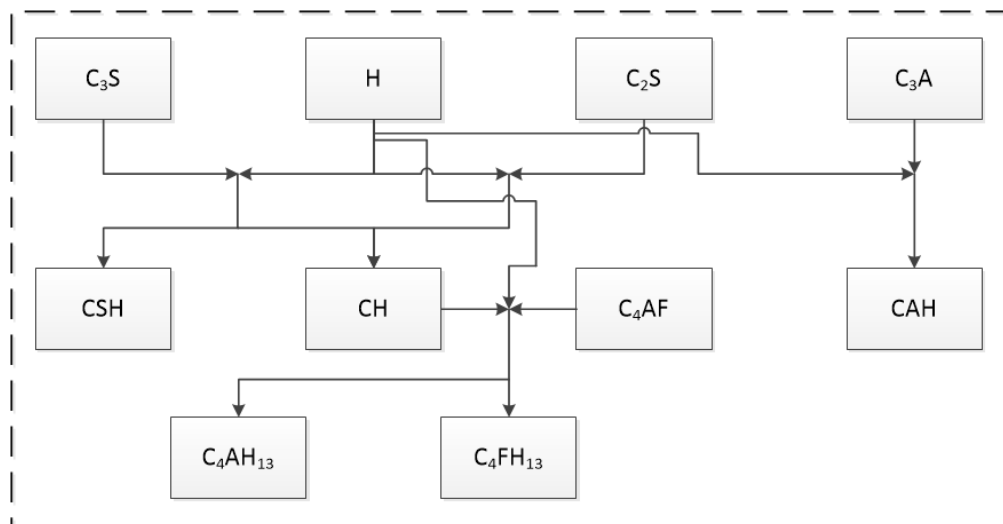



Figure 2. The cement hydration mechanism scheme.

	<b>Title</b> <b>Report on the assessment of the quality increase of cements enabled by the RECODE CO<sub>2</sub>-derived additives</b>	<b>Deliverable number</b> <b>D7.5</b>
		<b>Version</b> <b>Final</b>

### 3 Performance of CaCO<sub>3</sub> in cement mortars

#### 3.1 Characterization of the commercial CaCO<sub>3</sub>

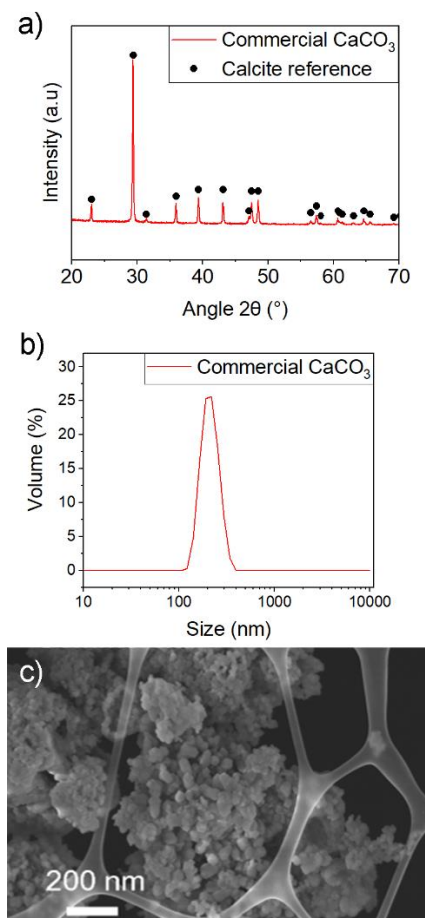



Figure 3. Commercial CaCO<sub>3</sub> particles characterization. a) X-Ray Diffraction; b) PSD; c) FESEM micrographs.

Figure 3 shows the characterization of the commercial CaCO<sub>3</sub> nanoparticles. The XRD spectrum showed in Figure 3 a) indicates pure calcite crystals according to the Powder Diffraction File PDF-2 of JCPDS. No presence of other crystalline phases, such as metastable aragonite or vaterite, was observed. The DLS measurement revealed that these calcite crystals had a narrow PSD with a mean particle size equal to 200 nm, as shown in Figure 3 b). Figure 3 c) displays a FESEM micrograph of the particles. The sample has primary crystals with a rhombohedral structure with a size equal to 60 nm. The FESEM analysis is in good agreement with the XRD spectra since they present the classical cubic morphology of calcite [13]–[16]. On the other hand, the size obtained through the DLS analysis (Figure 3 b)) differed from the size observed in the FESEM micrograph, probably because the formation of agglomerates by the primary crystals influences the DLS measurement.

	<b>Title</b> <b>Report on the assessment of the quality increase of cements enabled by the RECODE CO<sub>2</sub>-derived additives</b>	<b>Deliverable number</b> <b>D7.5</b>
		<b>Version</b> <b>Final</b>

### 3.2 Preparation of cement mortars

Ordinary Portland Cement of type II/A-LL and strength class 42.5 R, provided by Buzzi Unicem Group, was used. It conforms to the harmonized European standard EN 197-1 and displays the CE marking as required by European regulation 305/2011 (CPR). This cement contains 80-94% clinker and 6-20% limestone and a maximum of 5% minor constituents is permitted. Its physical and mechanical properties are shown in Table 1 and its chemical properties are shown in Table 2. A content of  $1350 \pm 5$  g of standard sand pre-packed in bag was used in each mixture with particle size distribution in accordance with the European Standard EN 196-1 (Table 3). Synthesized CaCO<sub>3</sub> through carbonation was investigated in cement mortars. In this study, commercial CaCO<sub>3</sub> nanoparticles provided by Tec Star S.r.l was also used with chemical and physical properties listed in Table 4.

*Table 1. Physical and mechanical properties of OPC*

Parameters		
Blaine specific surface	cm <sup>2</sup> /g	3100-4500
Initial setting time	min	> 130
Volume stability	min	≤ 10
Flow test	%	> 80
Compressive strength after curing for 2 days	MPa	> 25.0
Compressive strength after curing for 28 days	MPa	> 47.0

*Table 2. Chemical properties of OPC*

Parameters		
Sulfates SO <sub>3</sub>	%	< 3.7
Chlorides Cl <sup>-</sup>	%	< 0.08
Chromium VI soluble in water	ppm	≤ 2


*Table 3. Particle size distribution of the CEN Reference Sand*

Sieve analysis							
Square mesh size	mm	< 3.7	2.00	1.60	1.00	0.50	0.16
Cumulative sieve residue	%	< 0.08	0	7 ± 5	33 ± 5	67 ± 5	87 ± 5

*Table 4. Chemical and physical properties of commercial nano CaCO<sub>3</sub>*

Parameters		
Appearance	-	powder; white
Average particle size	nm	60
Crystal Phase	-	calcite
Purity	%	≥ 99
Tap density	g/cm <sup>3</sup>	0.777

The experimental campaign consists of two different ways for incorporating CaCO<sub>3</sub> nanoparticles into the cement mortars. Part of the cement content was replaced with commercial nano CaCO<sub>3</sub> in different percentages (1% CaCO<sub>3</sub>, 2% CaCO<sub>3</sub>, 3% CaCO<sub>3</sub>, 7% CaCO<sub>3</sub> subs.). Moreover, commercial nano CaCO<sub>3</sub> was

	<b>Title</b> <b>Report on the assessment of the quality increase of cements enabled by the RECODE CO<sub>2</sub>-derived additives</b>	<b>Deliverable number</b> <b>D7.5</b>
		<b>Version</b> <b>Final</b>

added to cement mortars according to the cement weight (7% CaCO<sub>3</sub> add.). The mixture proportions of the cement mortars are visible in Table 5. In addition, the three different polymorphs of synthesized CaCO<sub>3</sub>, i.e calcite, vaterite and aragonite were incorporated into the mixtures in two different substitution percentages (1%-2% Calc.; 1%-2% Vater.; 1%-2% Aragon.) with the intention of investigating the effect of the polymorphism on the mechanical performance of cement mortars.

In order to make the cement mortars, CaCO<sub>3</sub> slurry samples were prepared by gradually adding a known amount of CaCO<sub>3</sub> to a beaker containing a known amount of cold distilled water according to the mixture composition. The suspension was continuously mixed by means of ultrasonication using a VCX 750 sonicator & 13mm probe, with an 85% amplitude. The slurry sample and the cement were placed in a stainless-steel bowl and cement mortar mixtures were prepared in accordance with the European Standard EN 196-1 “Methods of testing cement - Part 1: Determination of strength” [17]. Finally, specimens were stored in a humid atmosphere for 24 hours, and once they were unpacked, they were immersed in water at (20.0 ±1.0) ° C for curing for 7 and 28 days.


*Table 5. Cement mortar mixtures proportion*

ID Mixture	OPC (g)	Water (g)	Standard Sand (g)	Nano CaCO <sub>3</sub> (g)
Mortar	450	225	1350	0
1% CaCO <sub>3</sub>	445.5	225	1350	4.5
2% CaCO <sub>3</sub>	441	225	1350	9.0
3% CaCO <sub>3</sub>	436.5	225	1350	13.5
7% CaCO <sub>3</sub> subs.	418.5	225	1350	31.5
7% CaCO <sub>3</sub> add.	450	225	1350	31.5
1% Calc.	445.5	225	1350	4.5
2% Calc.	441	225	1350	9.0
1% Vater.	445.5	225	1350	4.5
2% Vater.	441	225	1350	9.0
1% Aragon.	445.5	225	1350	4.5
2% Aragon.	441	225	1350	9.0

### 3.3 Mechanical test activity

Mechanical tests were carried out in accordance with the specifications given by European Standard EN 196-1 [17]. Specimens were subjected to Three-Point Bending test (TPB) using the Zwick Line-Z050 machine with a load cell of 50 kN (Figure 4). Compression test was carried out on halves of the specimens broken in TPB test using the Zwick Roell SMART PRO testing machine with a load cell of 1000 kN (Figure 5). Figure 6 a) and b) present results from mechanical testing on the experimental specimens containing commercial nano CaCO<sub>3</sub>. These results show that the mechanical properties of cementitious composites mainly depended on nano CaCO<sub>3</sub> contents. Results from the mechanical test activity showed that the flexural strength increased by 2.4%, 5.3%, 1.4% and 5.8% with the CaCO<sub>3</sub> substitution of 1, 2, 3 and 7% after 7 days of curing, thus indicating an acceleration in cement hydration employing CaCO<sub>3</sub> nanoparticles as nanofiller. The flexural strength rose by increasing the CaCO<sub>3</sub> substitution up to 2% after 28 days of curing. A higher filler content did not provide any further enhancement on the flexural strength of the specimens, which indicates that the filler effect of the CaCO<sub>3</sub> could be lost due to the aggregation of



	<b>Title</b> <b>Report on the assessment of the quality increase of cements enabled by the RECODE CO<sub>2</sub>-derived additives</b>	<b>Deliverable number</b> <b>D7.5</b>
		<b>Version</b> <b>Final</b>

crystals caused by great concentrations. In the 7% substitution with  $\text{CaCO}_3$ , there was a 5.6% decrease in the flexural strength in specimens tested. The results obtained from the compression tests are illustrated in Figure 6 b and indicate that the lowest substitution percentages (1%, 2%) with nano $\text{CaCO}_3$  provided good improvements in specimens in terms of compression strength after 7 and 28 days of curing. Parallel to the flexural tests, the higher substitution percentages of cement with nano $\text{CaCO}_3$  showed poor performance in compression tests. The flexural strength reduced with 3% substitution and then increased with 7% substitution after 7 days with respect to cement mortar without additive. This suggests that after 7 days, the  $\text{CaCO}_3$  effect on the hydration rate was weakened with 3% substitution, probably due to agglomeration issues that seriously reduce the specific surface of the filler. Despite the agglomeration problem, the compressive strength increased with higher filler contents. The 7% substitution with nano $\text{CaCO}_3$  improved compressive strength after 7 days of curing. After 28 days, 3 and 7% substitution reduced the compressive strength of the specimens with respect to cement mortar without additive.

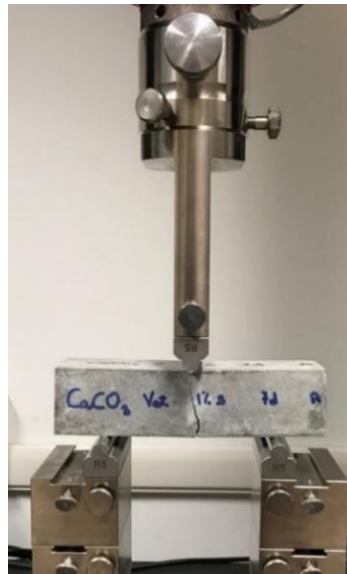


Figure 4. Three Point Bending test activity

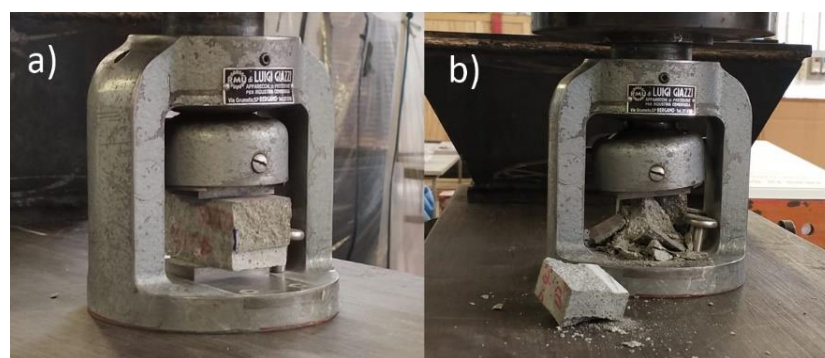



Figure 5. Compression test activity

	<b>Title</b> <b>Report on the assessment of the quality increase of cements enabled by the RECODE CO<sub>2</sub>-derived additives</b>	<b>Deliverable number</b> <b>D7.5</b>
		<b>Version</b> <b>Final</b>

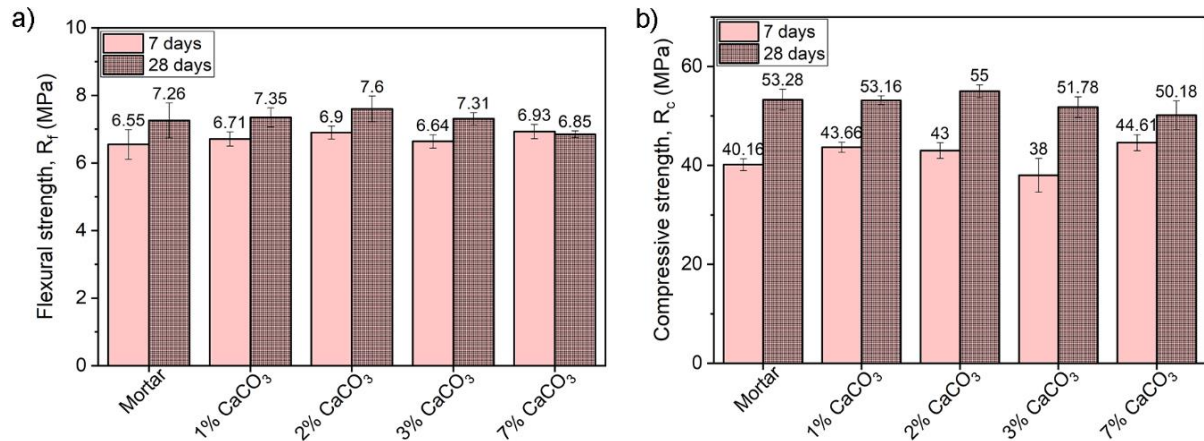


Figure 6. Cement mortars containing commercial nano  $\text{CaCO}_3$  in substitution of cement. a) Flexural strength (mean value) after 7 and 28 days of curing; b) Compressive strength (mean value) after 7 and 28 days of curing.

The substitution with  $\text{CaCO}_3$  was compared to the addition of  $\text{CaCO}_3$  in the cement mortar matrix by considering 7%. Figure 7 a) and b) show that  $\text{CaCO}_3$  added to cement mortars provided better mechanical strength than cement substitution by  $\text{CaCO}_3$ .  $\text{CaCO}_3$  used as nanofiller densified the structure of cement matrix by decreasing voids and pores, thus improving the strength and durability of the material. The cement content can be reasonably replaced with nanomaterials such as calcium carbonate. However, it is conceivable that a large amount of cement replacement corresponds to a reduction of strength performance of the cementitious materials, derived from the loss of adhesive and cohesive properties of the cement binder. The cement hydration was investigated through TGA and XRD analysis. Figure 8 a and b present the TGA curves of the cement mortar specimens after curing for 7 and 28 days, respectively.

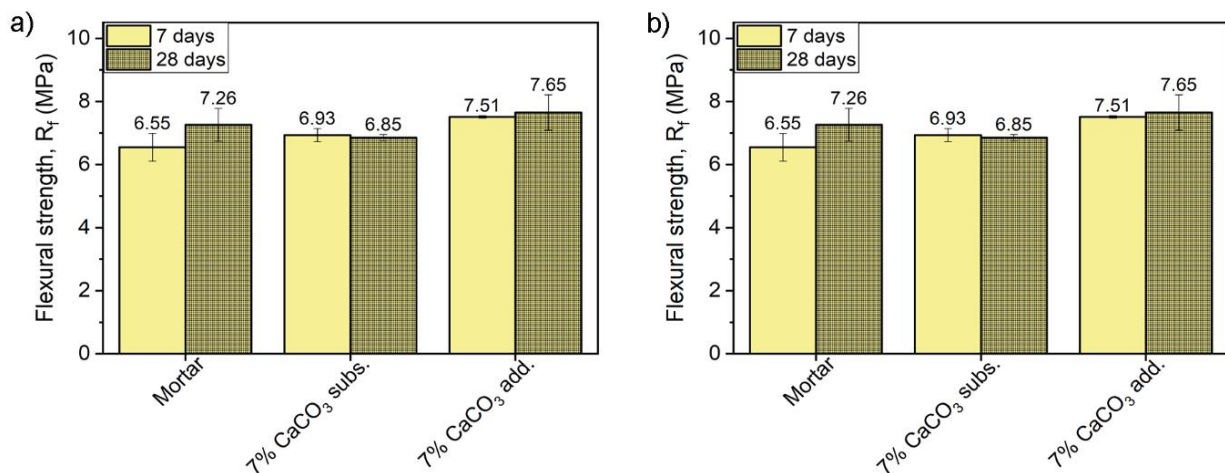



Figure 7. 7% substitution vs 7% addition of commercial nano  $\text{CaCO}_3$  in cement mortars. a) Flexural strength (mean value) after 7 and 28 days of curing; b) Compressive strength (mean value) after 7 and 28 days of curing.

	<b>Title</b> <b>Report on the assessment of the quality increase of cements enabled by the RECODE CO<sub>2</sub>-derived additives</b>	<b>Deliverable number</b> <b>D7.5</b>
		<b>Version</b> <b>Final</b>

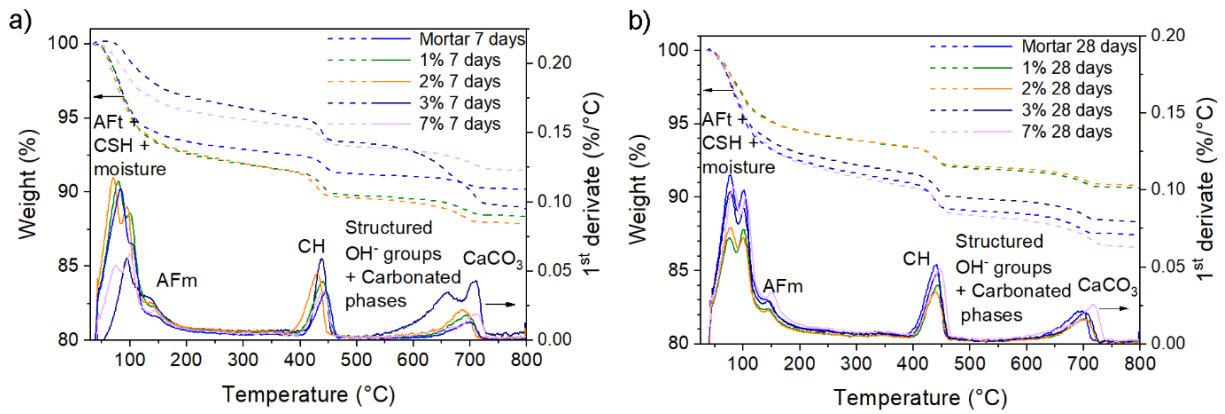


Figure 8. Thermogravimetric Analysis of cement mortar specimens: a) after 7 days of curing; b) after 28 days of curing.

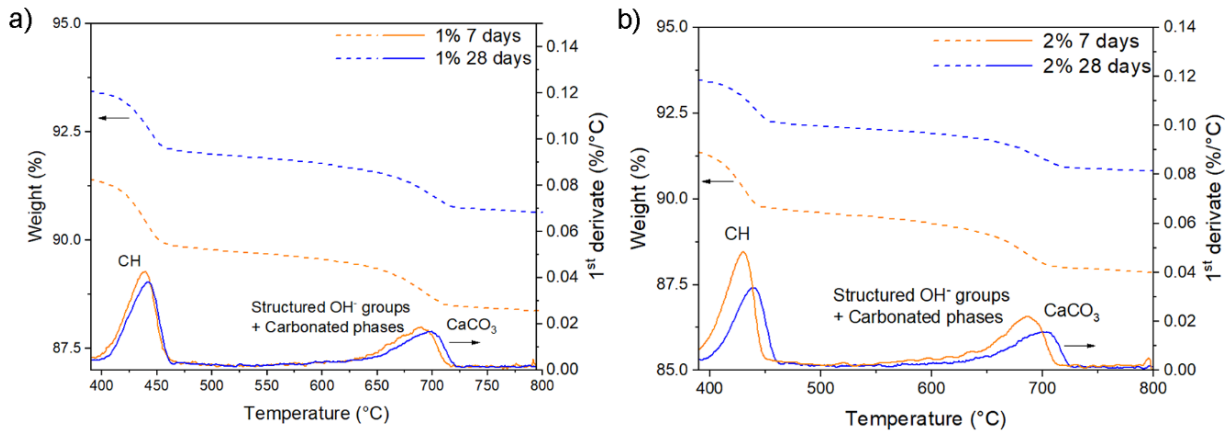



Figure 9. TGA-DTA profiles of CH dehydration and carbonated profiles decomposition of specimens containing: a) 1% nano-CaCO<sub>3</sub>; b) 2% nano-CaCO<sub>3</sub>.

Several peaks can be appreciated in the differential thermal analysis curve. The first peaks in the 100 °C - 125 °C interval correspond mainly to a water loss from the cement surface, CSH gel, and dehydration of ettringite (AFt). Then, a peak corresponding to monosulfate (AFm) around 145 °C. Calcium hydroxide (CH) degrades at 440 °C, while the last mass losses between 550 and 725 °C can be attributed to OH-groups, carbonated phases from CSH gel and CaCO<sub>3</sub>. These curves describe the characteristic shape of the hydrated cement [18].

Figure 9 illustrates the cement hydration progress. The peak corresponding to CH was broader for specimens cured for 7 days than for specimens cured for 28 days. After 28 days, this peak shifted to the right because of the transformation of portlandite into more crystallized forms [18]. CH peaks after 28 days also had a lower area, reflecting CH and C<sub>2</sub>AF transformation into C<sub>4</sub>AH<sub>13</sub> and C<sub>4</sub>FH<sub>13</sub> according to the mechanism shown in Figure 2, and the CH consumption through the pozzolanic reaction in the presence of water to make further CSH and CAH (eq. (1) and (2)). Moreover, the peaks of structured OH<sup>-</sup> and carbonated phases after 28 days of curing shifted to higher temperatures than after 7 days of curing for both cases, cement mortars containing 1% and 2% of nano CaCO<sub>3</sub>. These results indicate a further improvement of the CSH gel structure due to a longer hydration time and higher crystallization of carbonated phases [18].

	<b>Title</b> <b>Report on the assessment of the quality increase of cements enabled by the RECODE CO<sub>2</sub>-derived additives</b>	<b>Deliverable number</b> <b>D7.5</b>
		<b>Version</b> <b>Final</b>

Quantifying the content of Aft, AFm and CSH prove to be complex due to the fact that the peaks overlap. On the other hand, the content of calcium hydroxide (CH(%)) can be estimated according to the Taylor equation (eq. (1)) [7], [8].

$$CH (\%) = WL_{CH}(\%) \frac{MW_{CH}}{MW_w} \quad (1)$$

$WL_{CH}(\%)$  is the CH weight loss percentage,  $MW_{CH}$  and  $MW_w$  are the CH and water molar weights.

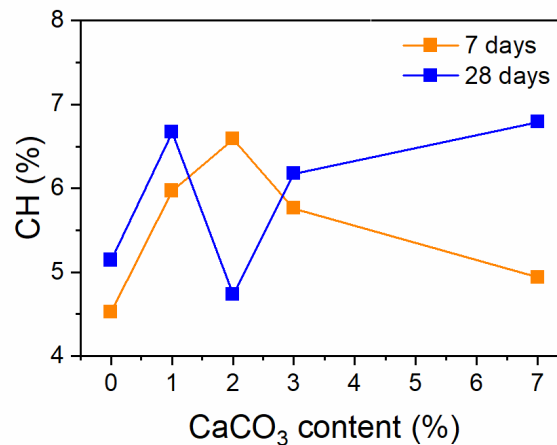



Figure 10. Calcium hydroxide (CH) of sample cement mortar and cement mortar containing nano CaCO<sub>3</sub>.

Figure 10 shows the CH content in cement mortars after curing for 7 and 28 days. After 7 days of curing, the specimens containing nano CaCO<sub>3</sub> had a higher CH content than sample mortars, indicating higher hydration rates at the early stages of curing. On the other hand, after 28 days of curing, the CH content was lower for specimens containing nano CaCO<sub>3</sub>. This indicates a higher CH consumption through pozzolanic reaction to form more CSH and CAH coupled to a further C<sub>4</sub>AF and CH hydration to form C<sub>4</sub>AH<sub>13</sub> and C<sub>4</sub>FH<sub>13</sub>. The further formation of CSH gel provides strength to the cement matrix, while the formation of C<sub>4</sub>AH<sub>13</sub> and C<sub>4</sub>FH<sub>13</sub> has no significant effect on the strength of hardened cementitious composites [9]. The CH content after 28 days increased for high CaCO<sub>3</sub> contents (3 and 7%), meaning lower CSH formation, which explains why compressive and flexural strengths were higher in the specimen containing 2% substitution of nano CaCO<sub>3</sub>, as seen in Figure 6. XRD spectra in Figure 11 display crystalline phases present in the sample cement mortars and the cement mortars with CaCO<sub>3</sub> nanoparticles after 7 and 28 days of curing. Like the TGA curves, the XRD spectra showed the typical characteristics peaks for a cured cementitious matrix, i.e. the expected hydration products, including calcium hydroxide (portlandite), ettringite (Aft), poorly crystallized CSH and unreacted clinker phases (mainly calcium silicate phases). Calcite (CaCO<sub>3</sub>) was not evident in the XRD analysis, unlike the TGA, probably due to the low content of calcite in the matrix. Alternatively, the calcite peak could overlap with the quartz peak at 2θ 29°. Quartz was the predominant crystalline phase in the specimens, confirming the high peak intensity at 21° and 26°. Incorporating CaCO<sub>3</sub> nanoparticles in the cement matrix resulted in a higher amount of hydrated product (CH and amorphous CSH) due to the acceleration of the hydration reaction. CH and CSH content

	<b>Title</b> <b>Report on the assessment of the quality increase of cements enabled by the RECODE CO<sub>2</sub>-derived additives</b>	<b>Deliverable number</b> <b>D7.5</b>
		<b>Version</b> <b>Final</b>

were instead undetectable in the cement mortar spectrum. By increasing the amount of CaCO<sub>3</sub> in the cement matrix, the rate of hydration reaction increased.

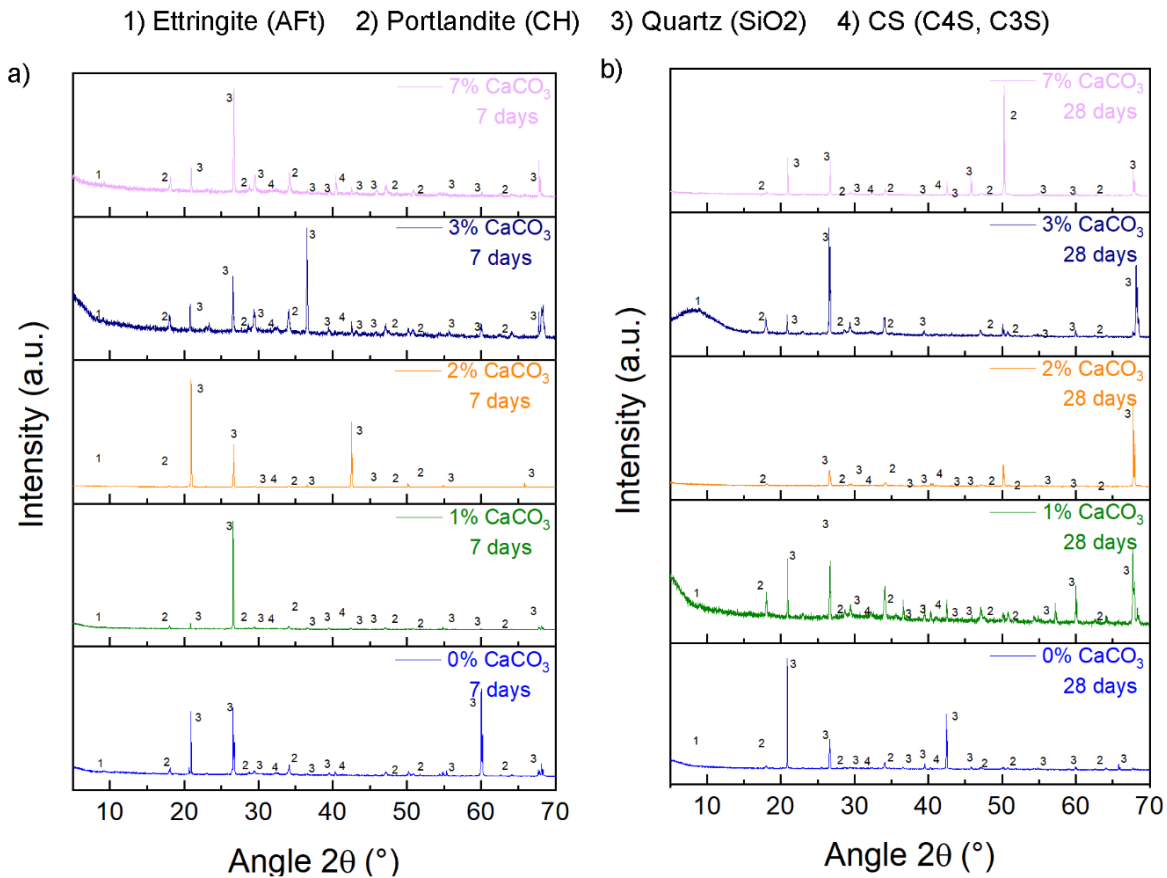



Figure 11. XRD pattern of cement mortars specimens: a) after 7 days of curing; b) after 28 days of curing.

Specimens with 1% and 2% of nano CaCO<sub>3</sub> exhibited a low quantity of hydrated products after 7 days, whereas specimens with 3% and 7% of nano CaCO<sub>3</sub> showed a higher content of hydrated products. XRD patterns of cement mortars after 28 days of curing showed a change in the crystalline structure of the cement than 7 days of curing, probably due to further pozzolanic reactions resulting in a high quantity of amorphous products (CSH). As seen in Figure 7, after 7 days, specimens containing 7% of nano CaCO<sub>3</sub> exhibited higher flexural and compressive strengths, indicating the fastest formation of hydrated compounds (CH) during the early curing stages compared to the other specimens. After 28 days, the CH peaks did not practically change with 7% of CaCO<sub>3</sub>, which mean a low transformation of CH into more hydrated species through the pozzolanic reactions. Instead, after 28 days of curing, the specimens with the best performance were those containing 2% of nano CaCO<sub>3</sub> (Figure 6), which presented low content of dehydrated calcium silicates (C<sub>2</sub>S and C<sub>3</sub>S) and low content of CH and quartz, thus highlighting the effect of pozzolanic reactions to form amorphous CSH. These findings suggest a correlation between the cement hydration process and the resulting mechanical properties of cementitious composites. The incorporation



	<b>Title</b> <b>Report on the assessment of the quality increase of cements enabled by the RECODE CO<sub>2</sub>-derived additives</b>	<b>Deliverable number</b> <b>D7.5</b>
		<b>Version</b> <b>Final</b>

of CaCO<sub>3</sub> nanoparticles in the cement matrix enhanced the hydration reaction. In the early stages of curing, the flexural and compressive strength of the cement mortars improved with the content of nano CaCO<sub>3</sub>. However, after 28 days of curing, the filler effect of the particles became more effective for the improvement of the mechanical properties, which may be reduced at higher filler concentrations.

### 3.4 CaCO<sub>3</sub> particles synthesized using the PBR

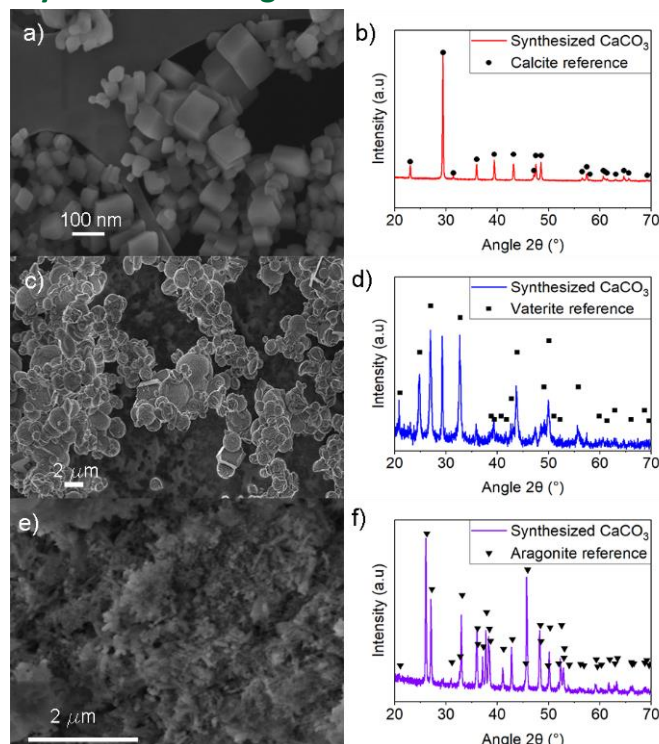


Figure 12. CaCO<sub>3</sub> crystals characterization: a) FESEM micrographs calcite crystals; b) XRD calcite crystals; c) FESEM micrographs vaterite crystals; d) XRD vaterite crystals; e) FESEM micrographs aragonite crystals; f) XRD aragonite crystals.

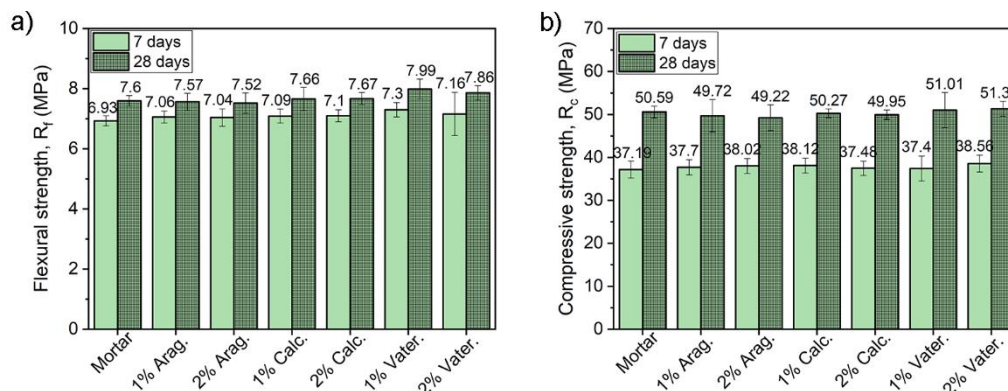



Figure 13. Cement mortars containing synthesized CaCO<sub>3</sub> in substitution of cement. Effect of crystal phase on: a) Flexural strength (mean value) after 7 and 28 days of curing; b) Compressive strength (mean value) after 7 and 28 days of curing.

	<b>Title</b> <b>Report on the assessment of the quality increase of cements enabled by the RECODE CO<sub>2</sub>-derived additives</b>	<b>Deliverable number</b> <b>D7.5</b>
		<b>Version</b> <b>Final</b>


The experimental work also envisaged incorporating CaCO<sub>3</sub> nanoparticles in cement mortars synthesized through carbonation using the PBR. The characterization of these crystals is shown in Figure 12. Sub-micron calcite crystals with a rhombohedral structure (See Figure 12 a and b), vaterite microparticles with a spherical structure (See Figure 12 c and d) and needle-like structured aragonite nanocrystals (See Figure 12 e and f) were employed as nanofiller in cement mortars. Figure 13 summarizes results obtained from the mechanical testing on cement mortars characterized by the partial replacement of cement content with the three different polymorphs of CaCO<sub>3</sub>, i.e. calcite, aragonite and vaterite. Figure 13 a reports results obtained from the TPB tests. A good performance was seen for synthesized CaCO<sub>3</sub> nanoparticles both after 7 and 28 days of curing. After 7 days, the flexural strength rose by 5.3% in specimens with 1% vaterite substitution and by 3.2% in specimens with 2% vaterite substitution compared to the reference samples. This trend was confirmed also after 28 days of curing. The other two types of crystals forms, aragonite and calcite, exhibited a good gain in terms of flexural strength after 7 days of curing. Figure 13 b shows results from the compression tests. After 7 days of curing, the compressive strength did not decrease on any occasion in cement mortars containing the CaCO<sub>3</sub> crystals with respect to the reference cement mortars. Instead, it increased up to around 4% in specimens containing 2% of substitution of cement with vaterite. By contrast, after 28 days of curing the compressive strength slightly decreased in the experimental specimens with aragonite and calcite crystals, up to 2.7% in the case of 2% of substitution of OPC with aragonite nanoparticles. The vaterite 2% substitution exhibited the best performance in compression tests after 28 days of curing.

To sum up, the optimal substitution percentage in cement mortars with vaterite proved to be 1% in TPB test and 2% in the compression test. The effect of the crystal phase on the mechanical properties of cementitious material was revealed. It seems that the sharp edges of the polygonal aragonite crystals had a lower filling effect, causing stress concentration, which made the specimen crack easily. The rhombohedral shape of the calcite crystals made it possible to obtain a small gain on the mechanical properties and fracture behaviour of the cement. The spherical vaterite crystals did not cause this stress concentration, leading to an improvement in the flexural and compressive strength of the cementitious materials with respect to a random polygonal filler.

These findings validate the numerical modelling study performed by Ouyang et al. [19], who suggested that the shape of the crystals has a significant effect on the mechanical performance of the cement. Furthermore, the filler-matrix interface strength seems to be the dominant influencing factor on the strength of the cement paste specimens. Therefore, the smaller size of the calcite crystals was expected to exhibit the best performance. However, the lower stability of vaterite could provide a stronger reactive effect during the hydration of the aluminium sulphated compounds in the cement matrix, as stated by Hargis et al. [20]. Coupled with this, the higher roughness presented by the vaterite particles compared to calcite particles could also positively influence the performance of the filler, according to work by Ouyang et al. [19]. All these aspects also reflect the higher performance of vaterite compared to the commercial nano CaCO<sub>3</sub>.

## 4 Performance of CaCO<sub>3</sub> in concrete

### 4.1 Materials and methods

	<b>Title</b> <b>Report on the assessment of the quality increase of cements enabled by the RECODE CO<sub>2</sub>-derived additives</b>	<b>Deliverable number</b> <b>D7.5</b>
		<b>Version</b> <b>Final</b>

Concrete mixtures containing nano-CaCO<sub>3</sub> were designed to determine the optimal proportions of all their components (their density is given in Table 6). Ordinary Portland Cement, type II/A-LL with the strength class 42.5 R, provided by the Buzzi Unicem Group, was used. Its physical and mechanical properties are listed in Table 1 and its chemical properties are shown in Table 2. The superplasticizer Dynamon SP1, provided by MAPEI S.p.A., was added to the mixtures in a percentage equal to 0.8 according to the cement weight (% wt). Its technical data are listed in

Table 7. Fine and coarse natural aggregates produced by I.L.C. S.r.l. were employed. Figure 14 plots the granulometric analysis curves of each aggregate, while Figure 15 compares the optimal resulting granulometric curve used with the theoretical Dreux curve. In Table 8 the optimal aggregate proportions determined for the concrete mix design are presented. The maximum diameter for the natural aggregates was 14 mm. A quantity of 185 kg/m<sup>3</sup> of water was used.

In total, twelve different concrete mixes were designed. Two pillar mixtures of concrete were considered:

- a concrete mix with a dosage of cement equal to 300 kg/m<sup>3</sup> (mix designation: M1)
- a concrete mix with a dosage of cement equal to 400 kg/m<sup>3</sup> (mix designation: M2).

The commercial nano-CaCO<sub>3</sub>, provided by Tec Star S.r.l., (see Table 4) was incorporated into the concrete mixtures in two different ways. Firstly, the CaCO<sub>3</sub> nano-filler was added to the mixes in different percentages (1%, 3% and 7%) according to the cement weight (see

Table 9 and Table 11). In the second part of the experimental campaign, part of the cement content was substituted with CaCO<sub>3</sub> nanoparticles in different percentages (1%, 3% and 7%) according to the cement weight (see


Table 10 and

Table 12).

The different concrete mixtures were named as follows:

- M1\_T: Concrete (cement dosage = 300 kg/m<sup>3</sup>) without nano-CaCO<sub>3</sub>
- M1\_F1%: Concrete (cement dosage = 300 kg/m<sup>3</sup>) with 1% addition of nano-CaCO<sub>3</sub>
- M1\_F3%: Concrete (cement dosage = 300 kg/m<sup>3</sup>) with 3% addition of nano-CaCO<sub>3</sub>
- M1\_F1%S: Concrete (cement dosage = 300 kg/m<sup>3</sup>) with 1% cement replaced with nano-CaCO<sub>3</sub>
- M1\_F3%S: Concrete (cement dosage = 300 kg/m<sup>3</sup>) with 3% cement replaced with nano-CaCO<sub>3</sub>
- M2\_T: Concrete (cement dosage = 400 kg/ m<sup>3</sup>) without nano-CaCO<sub>3</sub>
- M2\_F1%: Concrete (cement dosage = 400 kg/ m<sup>3</sup>) with 1% addition of nano-CaCO<sub>3</sub>
- M2\_F3%: Concrete (cement dosage = 400 kg/ m<sup>3</sup>) with 3% addition of nano-CaCO<sub>3</sub>
- M2\_F7%: Concrete (cement dosage = 400 kg/ m<sup>3</sup>) with 7% addition of nano-CaCO<sub>3</sub>
- M2\_F1%S: Concrete (cement dosage = 400 kg/ m<sup>3</sup>) with 1% cement replaced with nano-CaCO<sub>3</sub>
- M2\_F3%S: Concrete (cement dosage = 400 kg/ m<sup>3</sup>) with 3% cement replaced with nano-CaCO<sub>3</sub>
- M2\_F7%S: Concrete (cement dosage = 400 kg/ m<sup>3</sup>) with 7% cement replaced with nano-CaCO<sub>3</sub>



	<b>Title</b> <b>Report on the assessment of the quality increase of cements enabled by the RECODE CO<sub>2</sub>-derived additives</b>	<b>Deliverable number</b> <b>D7.5</b>
		<b>Version</b> <b>Final</b>

Three mixtures (volume: 30 lt) were made for each concrete mix type. In general, from each mix type, three cubes for penetration tests, three prismatic specimens for three-point bending tests and at least two cubic specimens for compression tests at 7 and 28 days after curing were made.

*Table 6. Density of the concrete mix components*


Mix Components		Density
Air	Mg/m <sup>3</sup>	-
Water	Mg/m <sup>3</sup>	1.00
Cement	Mg/m <sup>3</sup>	3.15
Superplasticizer	Mg/m <sup>3</sup>	1.08
CaCO <sub>3</sub>	Mg/m <sup>3</sup>	2.70

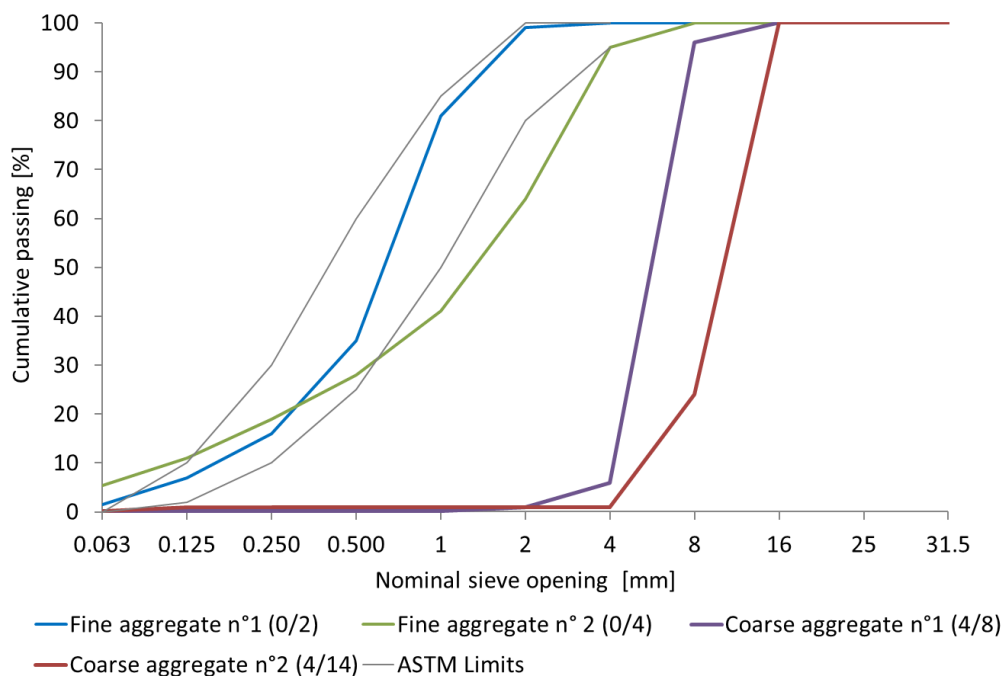


*Figure 14. Granulometric analysis curves of each aggregate of concrete mix*

*Table 7. Technical data of Mapei Dynamon SP1*

Parameters		Values
Consistency	-	liquid
Colour	-	amber
Density	g/m <sup>3</sup>	1.08 ± 0.02 at 20°C
Chlorides soluble in water	%	< 0.1

	<b>Title</b> <b>Report on the assessment of the quality increase of cements enabled by the RECODE CO<sub>2</sub>-derived additives</b>	<b>Deliverable number</b> <b>D7.5</b>
		<b>Version</b> <b>Final</b>

<b>Alkali content</b>	%	< 3.0
<b>pH</b>	-	6.5 ± 1.0

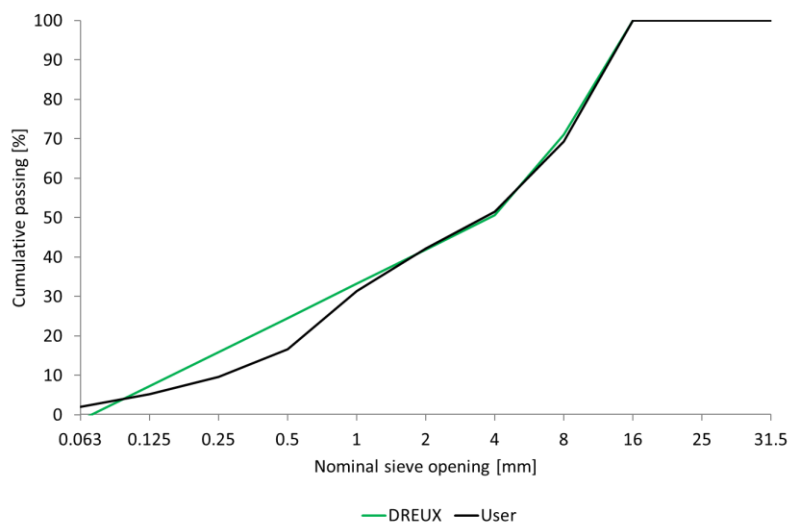


Figure 15. Granulometric analysis curve used vs theoretical Dreux curve

Table 8. Aggregate proportions for concrete mix design


Aggregate type (d/D)		Proportions
Fine aggregate n°1 (0/2)	%	24
Fine aggregate n° 2 (0/4)	%	28
Coarse aggregate n° 1 (4/8)	%	8
Coarse aggregate n° 2 (4/14)	%	40

Table 9. Main features of the concrete mixtures M1 with CaCO<sub>3</sub> addition

Main Mix Features		M1_T	M1_1%	M1_3%
Cement dosage	kg/m <sup>3</sup>	300	300	300
Additive dosage	% wt	0.8	0.8	0.8
CaCO <sub>3</sub> dosage	% wt	0	1.0	3.0
Consistency class	-	S4	S4	S4
Water/Cement	-	0.62	0.62	0.62
Aggregate D <sub>max</sub>	mm	14	14	14
Entrained Air	%	2	2	2

Table 10. Main features of the concrete mixtures M1 with CaCO<sub>3</sub> substitution

Main Mix Features		M1_T	M1_F15%	M1_F35%
Cement dosage	kg/m <sup>3</sup>	300	297	291

	<b>Title</b> <b>Report on the assessment of the quality increase of cements enabled by the RECODE CO<sub>2</sub>-derived additives</b>	<b>Deliverable number</b> <b>D7.5</b>
		<b>Version</b> <b>Final</b>

<b>Additive dosage</b>	% wt	0.8	0.8	0.8
<b>CaCO<sub>3</sub> dosage</b>	% wt	0	1.0	3.0
<b>Consistency class</b>	-	S4	S4	S4
<b>Water/Cement</b>	-	0.62	0.62	0.62
<b>Aggregate D<sub>max</sub></b>	mm	14	14	14
<b>Entrained Air</b>	%	2	2	2

*Table 11. Main features of the concrete mixtures M2 with CaCO<sub>3</sub> addition*

<b>Main Mix Features</b>		<b>M2_T</b>	<b>M2_F1%</b>	<b>M2_F3%</b>	<b>M2_F7%</b>
<b>Cement dosage</b>	kg/m <sup>3</sup>	400	400	400	400
<b>Additive dosage</b>	% wt	0.8	0.8	0.8	0.8
<b>CaCO<sub>3</sub> dosage</b>	% wt	0	1.0	3.0	7.0
<b>Consistency class</b>	-	S4	S4	S4	S4
<b>Water/Cement</b>	-	0.46	0.46	0.46	0.46
<b>Aggregate D<sub>max</sub></b>	mm	14	14	14	14
<b>Entrained Air</b>	%	2	2	2	2

*Table 12. Main features of the concrete mixtures M2 with CaCO<sub>3</sub> substitution*

<b>Main Mix Features</b>		<b>M2_T</b>	<b>M2_F1S%</b>	<b>M2_F3S%</b>	<b>M2_F7S%</b>
<b>Cement dosage</b>	kg/m <sup>3</sup>	400	396	388	372
<b>Additive dosage</b>	% wt	0.8	0.8	0.8	0.8
<b>CaCO<sub>3</sub> dosage</b>	% wt	0	1.0	3.0	7.0
<b>Consistency class</b>	-	S4	S4	S4	S4
<b>Water/Cement</b>	-	0.46	0.46	0.46	0.46
<b>Aggregate D<sub>max</sub></b>	mm	14	14	14	14
<b>Entrained Air</b>	%	2	2	2	2


Slump tests were performed on the fresh concrete to evaluate its workability in accordance with the specifications given in EN 12350-2 “Testing fresh concrete - Part 2: Slump Test” [21]. Immediately after the mixing process, the fresh concrete was poured into and then compacted in a truncated conical mould. The concrete cone slumped, and the distance it slumped thus provided a measure of the concrete consistency (see Figure 17).

The density of the compacted fresh concrete was determined in accordance with the specifications given in EN 12350-6 “Testing fresh concrete - Part 6: Density” [22]. The density was calculated using the following equation (eq. 3):

$$D = \frac{m_2 - m_1}{V} \quad \left[ \frac{kg}{m^3} \right] \quad (2)$$

where D is the density of the fresh concrete [kg/m<sup>3</sup>]; m<sub>1</sub> is the mass of the empty density container [kg]; m<sub>2</sub> is the mass of the density container filled with the compacted concrete [kg]; V is the volume of the density container [m<sup>3</sup>].

Compression tests were carried out (see Figure 19) with the Galdabini servo-controlled compact compression testing machine to determine the compressive strength of the hardened concrete cubes in accordance with the specifications given in EN 12390-3 “Testing hardened concrete - Part 3: Compressive

	<b>Title</b> <b>Report on the assessment of the quality increase of cements enabled by the RECODE CO<sub>2</sub>-derived additives</b>	<b>Deliverable number</b> <b>D7.5</b>
		<b>Version</b> <b>Final</b>

strength of test specimens” [23]. The tests were performed at 7 and 28 days after curing (see Figure 18). The compressive strength was calculated using the following equation (eq. 4):

$$f_c = F/A_c \text{ [MPa]} \quad (3)$$


where  $f_c$  is the compressive strength [MPa],  $F$  is the maximum load [N],  $A_c$  is the cross-sectional area of the specimen on which the compressive force acts [mm<sup>2</sup>].

Three 28 day-cured cubic specimens for each concrete mix were subjected to water permeability testing (Figure 20) according to the European Standard EN 12390-8 “Testing hardened concrete - Part 8: Depth of penetration of water under pressure” [24]. The specimens were placed in the apparatus and a water pressure of  $(500 \pm 50)$  kPa was applied for  $(72 \pm 2)$  h. The appearance of the surfaces was monitored during the test to detect any water leakage. At the end of the test, the specimens were split in half, perpendicularly to the face on which the water pressure was applied. The water penetration front could be clearly seen on the split face, and it was marked, as shown in Figure 21. The maximum depth of penetration was recorded and measured to the nearest millimetre.

Three-point bending tests on some 150x150x600 mm prismatic specimens of concrete were carried out (see Figure 22). A single notch with a depth of 25 mm was made in the mid-span of the specimens. The tests were performed by means of the Crack Mouth Open Displacement (CMOD) control. The CMOD increases at the constant rate of 0.05 mm/min until the end of the test. The flexural tensile behaviour and fracture energy of the concrete specimens were analysed.



*Figure 16. Concrete mixtures cast*

	<b>Title</b> <b>Report on the assessment of the quality increase of cements enabled by the RECODE CO<sub>2</sub>-derived additives</b>	<b>Deliverable number</b> <b>D7.5</b>
		<b>Version</b> <b>Final</b>



*Figure 17. Slump test on the fresh concrete*



*Figure 18. Concrete specimens curing*




	Title <b>Report on the assessment of the quality increase of cements enabled by the RECODE CO<sub>2</sub>-derived additives</b>	Deliverable number <b>D7.5</b>
		Version <b>Final</b>



Figure 19. Compression test on the hardened concrete



Figure 20. Test of the depth of penetration of water under pressure on the hardened concrete


	<b>Title</b> <b>Report on the assessment of the quality increase of cements enabled by the RECODE CO<sub>2</sub>-derived additives</b>	<b>Deliverable number</b> <b>D7.5</b>
		<b>Version</b> <b>Final</b>




Figure 21. Marked front of water penetration in a concrete specimen with 3% of CaCO<sub>3</sub> addition.



Figure 22. Three-point bending test on the hardened concrete

## 4.2 Results and discussion

The concrete mixtures exhibited slumps in the consistency class S4, corresponding to slumps between 160 mm and 210 mm. The measurement of the slumps is presented in Table 13. The slumps slightly decreased

	<b>Title</b> <b>Report on the assessment of the quality increase of cements enabled by the RECODE CO<sub>2</sub>- derived additives</b>	<b>Deliverable number</b> <b>D7.5</b>
		<b>Version</b> <b>Final</b>


with the addition of nano-CaCO<sub>3</sub> to the concrete mixtures. Nanofillers can positively affect the mechanical and durability properties of hardened cementitious composites but may influence their workability [25]. The large specific surface of nanoparticles due to their small size increases the water demand of the concrete mix [26].

*Table 13. Slump tests measurement on the fresh concrete*

ID Mixtures	Slump [cm]	Standard	Density [kg/m <sup>3</sup> ]	Standard	D <sub>theor.</sub> /D <sub>real</sub>
M1_T	20	EN 12350-2	2448	EN 12350-6	0.984
M1_F1%	18	EN 12350-2	2452	EN 12350-6	0.982
M1_F3%	18	EN 12350-2	2450	EN 12350-6	0.983
M1_T	20	EN 12350-2	2444	EN 12350-6	0.997
M1_F1S%	20	EN 12350-2	2440	EN 12350-6	0.986
M1_F3S%	19	EN 12350-2	2438	EN 12350-6	0.984
M2_T	20	EN 12350-2	2460	EN 12350-6	0.984
M2_F1%	18	EN 12350-2	2450	EN 12350-6	0.988
M2_F3%	18	EN 12350-2	2460	EN 12350-6	0.984
M2_F7%	16	EN 12350-2	2470	EN 12350-6	0.980
M2_F1S%	20	EN 12350-2	2458	EN 12350-6	0.983
M2_F3S%	19	EN 12350-2	2452	EN 12350-6	0.978
M2_F7S%	18	EN 12350-2	2460	EN 12350-6	0.972

With regard to the pillar concrete mix M1, after 7 days of curing the compressive strength rose by 8% in the concrete specimens with the addition of 1% of the CaCO<sub>3</sub> nanofiller compared to the reference specimens. After 28 days of curing, there was a 6% increase (see Figure 26). The addition percentage of 3% of nano-CaCO<sub>3</sub> did not exhibit a significant gain compared to the reference samples (Figure 26). With regard to the pillar concrete mix M2, the 1% addition of nano-CaCO<sub>3</sub> noticeably improved the compressive strength both after 7 days and 28 days of curing (5% and 7% respectively). By contrast, the 3% percentage addition of nano-CaCO<sub>3</sub> showed poor performance in compression tests after 7 days (see Figure 27). The substitution of the cement powder with CaCO<sub>3</sub> nanoparticles in the M1 concrete mixtures caused a small decrease in the mechanical strength of the specimens (up to -4% in the specimens with 3% addition after 7 days of curing) as shown in Figure 24. There was no a significant gain of the compressive strength in the specimens made with the substitution of cement with nano-CaCO<sub>3</sub> in the M2 concrete mixtures (see Figure 25). Figure 23 illustrates the results from the compression tests performed on the M2 concrete mixes with a 7% addition of nano-CaCO<sub>3</sub> versus a 7% substitution of nano-CaCO<sub>3</sub>. The highest performance was exhibited by the specimens characterized by the addition of the nanofiller (up to 10% after 7 days of curing and 6% after 28 days of curing). Nonetheless, the incorporation of nano-CaCO<sub>3</sub> resulted in the boosted development of the compressive strength of the concrete at early age. These findings support the partly chemical and partly physical valuable effect of CaCO<sub>3</sub> when used as nanofiller in cementitious materials.



	<b>Title</b> <b>Report on the assessment of the quality increase of cements enabled by the RECODE CO<sub>2</sub>-derived additives</b>	<b>Deliverable number</b> <b>D7.5</b>
		<b>Version</b> <b>Final</b>

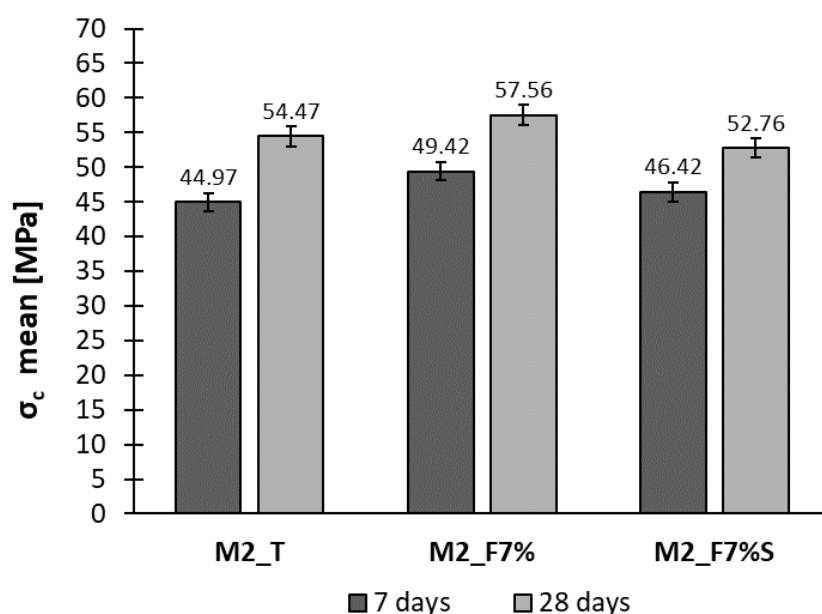


Figure 23. The compressive strength at 7 and 28 days after curing - mixture M2 with CaCO<sub>3</sub> addition and substitution vs reference mortars

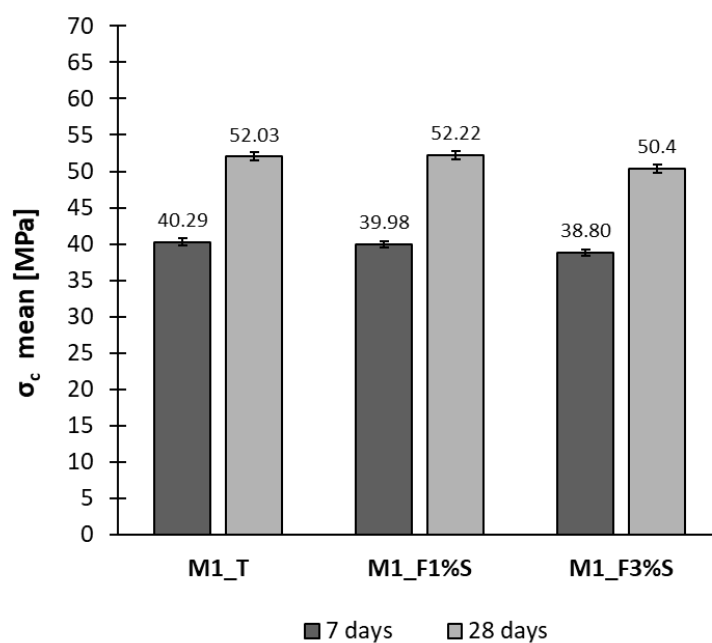



Figure 24. The compressive strength at 7 and 28 days after curing - mixture M1 with CaCO<sub>3</sub> substitution vs reference mortars

	<b>Title</b> <b>Report on the assessment of the quality increase of cements enabled by the RECODE CO<sub>2</sub>-derived additives</b>	<b>Deliverable number</b> <b>D7.5</b>
		<b>Version</b> <b>Final</b>

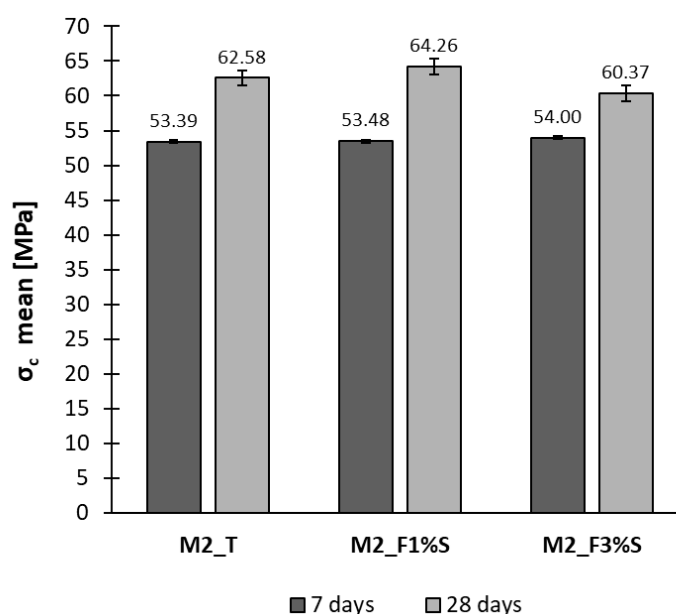


Figure 25. The compressive strength at 7 and 28 days after curing - mixture M2 with CaCO<sub>3</sub> substitution vs reference mortars

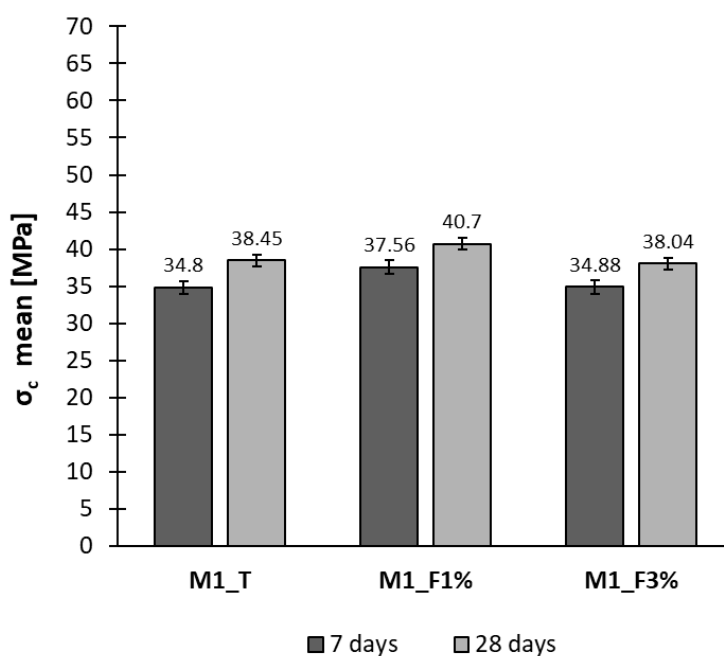



Figure 26. The compressive strength at 7 and 28 days after curing - mixture M1 with CaCO<sub>3</sub> addition vs reference mortars

	<b>Title</b> <b>Report on the assessment of the quality increase of cements enabled by the RECODE CO<sub>2</sub>-derived additives</b>	<b>Deliverable number</b> <b>D7.5</b>
		<b>Version</b> <b>Final</b>

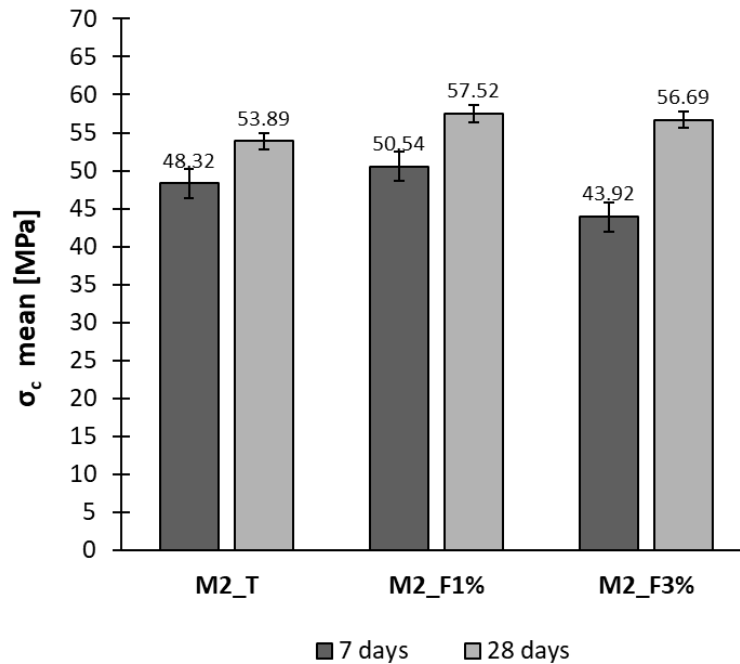



Figure 27. The compressive strength at 7 and 28 days after curing - mixture M2 with CaCO<sub>3</sub> addition vs reference mortars

The results from the tests of the depth of the penetration of water under pressure are shown in Table 14. The maximum depth of water penetration (evaluated as the mean value on three test specimens) is provided. The highest value recorded is below 30 mm. Generally, this value was lower in the specimens containing nano-filler compared to the concrete without it. The concrete mixtures characterized by 1% and 7% addition of nano-CaCO<sub>3</sub> showed less permeability, presumably linked to a reduction in the number and size of the cavities due to a good workability of the concrete mixes. This represents a good result since permeability is linked to the durability of concrete due to the access of water, carbon dioxide, chloride, sulphate, and other damaging substances.

The Load-CMOD curves obtained from the TPB tests are presented in Figure 28. Firstly, these curves have an elastic behavior. Secondly, an inelastic phase occurs, which corresponds to the initial growth of the microcracks, until the final load capacity of the specimen is reached, well-known as the peak load. After the peak load-point, since concrete is an almost brittle material, the specimens is damaged due to the coalescence of microcracks [27]. In fact, after the peak load-point, these curves show a decreasing trend. However, the post-peak response of the concrete mixtures made with the partial replacement of the cement content with commercial CaCO<sub>3</sub> seems to be very gradual. A small difference can be seen regarding the fracture properties of the concrete specimens.

Table 14. The maximum depth of water penetration (evaluated as the mean value on three test specimens) is provided. The highest value recorded is below 30 mm. Generally, this value was lower in the specimens containing nano-filler compared to the concrete without it. The concrete mixtures characterized by 1% and 7% addition of nano-CaCO<sub>3</sub> showed less permeability, presumably linked to a reduction in the number and size of the cavities due to a good workability of the concrete mixes. This represents a good result since permeability is linked to the durability of concrete due to the access of water, carbon dioxide, chloride, sulphate, and other damaging substances.


The Load-CMOD curves obtained from the TPB tests are presented in Figure 28. Firstly, these curves have an elastic behavior. Secondly, an inelastic phase occurs, which corresponds to the initial growth of the microcracks, until the final load capacity of the specimen is reached, well-known as the peak load. After the peak load-point, since concrete is an almost brittle material, the specimens is damaged due to the coalescence of microcracks [27]. In fact, after the peak load-point, these curves show a decreasing trend.

	<b>Title</b> <b>Report on the assessment of the quality increase of cements enabled by the RECODE CO<sub>2</sub>-derived additives</b>	<b>Deliverable number</b> <b>D7.5</b>
		<b>Version</b> <b>Final</b>

However, the post-peak response of the concrete mixtures made with the partial replacement of the cement content with commercial CaCO<sub>3</sub> seems to be very gradual. A small difference can be seen regarding the fracture properties of the concrete specimens.

*Table 14. Results from permeability tests on hardened concrete*

<b>Mixtures</b>	<b>Maximum Penetration [mm]</b>	<b>Standard</b>
<b>M1_T</b>	26	EN 12390-8
<b>M1_F1%</b>	18	EN 12390-8
<b>M1_F3%</b>	20	EN 12390-8
<b>M1_F1S%</b>	24	EN 12390-8
<b>M1_F3S%</b>	26	EN 12390-8
<b>M2_T</b>	25	EN 12390-8
<b>M2_F1%</b>	16	EN 12390-8
<b>M2_F3%</b>	27	EN 12390-8
<b>M2_F7%</b>	18	EN 12390-8
<b>M2_F1S%</b>	22	EN 12390-8
<b>M2_F3S%</b>	25	EN 12390-8
<b>M2_F7S%</b>	23	EN 12390-8

	<b>Title</b> <b>Report on the assessment of the quality increase of cements enabled by the RECODE CO<sub>2</sub>-derived additives</b>	<b>Deliverable number</b> <b>D7.5</b>
		<b>Version</b> <b>Final</b>

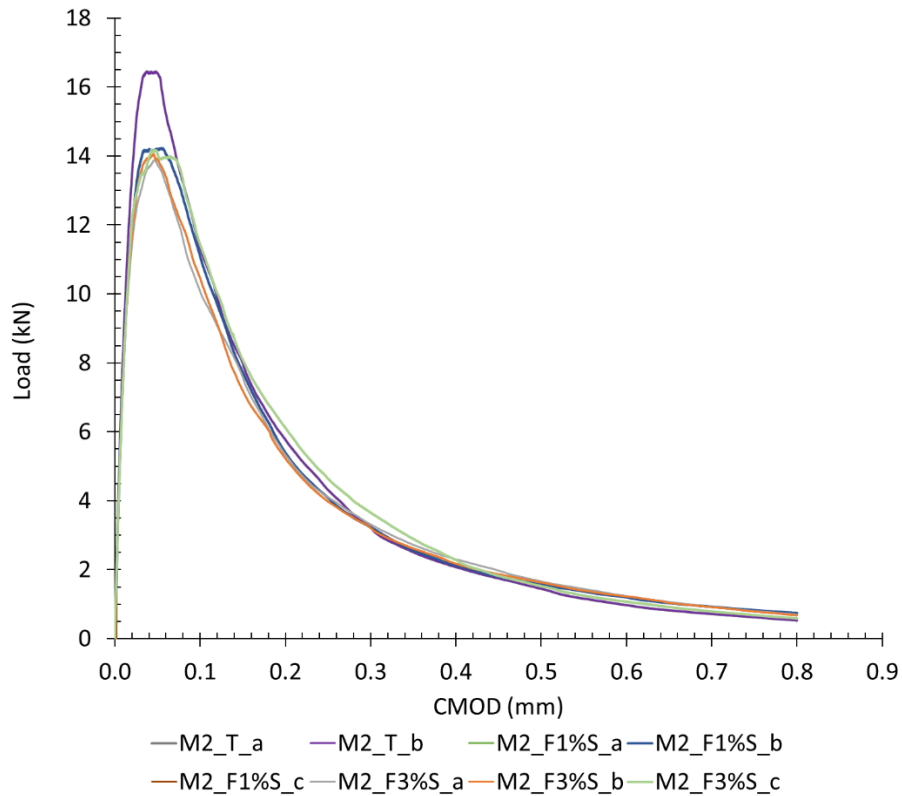



Figure 28. The Load-CMOD curves from TPB tests on the concrete prismatic specimens

## 5 Conclusions

The synthesis of  $\text{CaCO}_3$  through carbonation using the PBR was successfully studied. The calcite, aragonite and vaterite crystals were incorporated into the cement mortars as partial replacement of the cement content to investigate their effect on the mechanical properties of the cement mortars. Results showed that the 1% and 2% substitution of the cement content with the three types of polymorphism of  $\text{CaCO}_3$  provided a general enhancement of the flexural and compressive strength of the cementitious materials. In this study, commercial  $\text{CaCO}_3$  nanoparticles, provided by Tec Star S.r.l, with physical and chemical properties similar to those of the synthesized nanoparticles, were also incorporated into the cement mortars with the aim of creating a benchmark for a deeper investigation. The mechanical properties of commercial  $\text{CaCO}_3$  nanoparticles mainly depended on nano  $\text{CaCO}_3$  content. The flexural strength increased after 7 days of curing, thus indicating an acceleration in cement hydration with  $\text{CaCO}_3$  nanoparticles. After 28 days of curing, a higher  $\text{CaCO}_3$  content did not provide any further enhancement on the flexural strength of the specimens. The filler effect of the nanoparticles may have been lost due to the aggregation phenomena. The lowest substitution percentages (1%, 2%) with nano  $\text{CaCO}_3$  provided good improvements of compression strength after 7 and 28 days of curing. Parallel to the flexural tests, the higher substitution percentages of nano  $\text{CaCO}_3$  showed poor performance in compression tests.


	<b>Title</b> <b>Report on the assessment of the quality increase of cements enabled by the RECODE CO<sub>2</sub>-derived additives</b>	<b>Deliverable number</b> <b>D7.5</b>
		<b>Version</b> <b>Final</b>

Furthermore, the substitution with CaCO<sub>3</sub> was compared to the addition of CaCO<sub>3</sub> in the cement mortars by considering 7%. The cement mortars with the addition of CaCO<sub>3</sub> displayed better mechanical strength than cement mortars with substitution with CaCO<sub>3</sub>. However, the synthesized vaterite crystals exhibited the best performance as nanofiller thanks to their shape and roughness, providing a better filling effect. Besides, their lower stability enhanced the cement hydration kinetics.


The experimental campaign also envisaged the incorporation into different concrete mixtures of the commercial CaCO<sub>3</sub> nanoparticles. These commercial nanoparticles were used since the productivity of the synthesized nanoparticles at laboratory scale was too low (<10 g/d). The design of the concrete mixtures concerned the addition of these nanoparticles to the mixes as well as the partially replacement of the cement powder with the particles in different percentages (1,2,3,7%) according to the cement weight. Slumps and density were evaluated on the fresh concrete. Compression, depth of penetration of water under pressure and TPB tests were carried out on the hardened concrete. The concrete specimens exhibited a good performance, also in terms of permeability which is linked to the important durability properties of the material.

## References

- [1] E. Batuecas, F. Liendo, T. Tommasi, S. Bensaid, F. A. Deorsola, and D. Fino, "Recycling CO<sub>2</sub> from flue gas for CaCO<sub>3</sub> nanoparticles production as cement filler: A Life Cycle Assessment," *J. CO<sub>2</sub> Util.*, vol. 45, no. January, p. 101446, 2021, doi: 10.1016/j.jcou.2021.101446.
- [2] A. Hakamy, "Effect of CaCO<sub>3</sub> nanoparticles on the microstructure and fracture toughness of ceramic nanocomposites," *J. Taibah Univ. Sci.*, vol. 14, no. 1, pp. 1201–1207, 2020, doi: 10.1080/16583655.2020.1809840.
- [3] G. Ramakrishna and T. Sundararajan, *A novel approach to rheological and impact strength of fibre-reinforced cement/cementitious composites for durability evaluation*. Elsevier Ltd, 2018.
- [4] J. Camiletti, A. M. Soliman, and M. L. Nehdi, "Effects of nano- and micro-limestone addition on early-age properties of ultra-high-performance concrete," *Mater. Struct. Constr.*, vol. 46, no. 6, pp. 881–898, 2013, doi: 10.1617/s11527-012-9940-0.
- [5] L. McDonald, F. P. Glasser, and M. S. Imbabi, "A new, carbon-negative precipitated calcium carbonate admixture (PCC-A) for low carbon Portland cements," *Materials (Basel)*, vol. 12, no. 2, 2019, doi: 10.3390/ma12040554.
- [6] S. W. M. Supit and F. U. A. Shaikh, "Effect of Nano-CaCO<sub>3</sub> on compressive strength development of high volume fly ash mortars and concretes," *J. Adv. Concr. Technol.*, vol. 12, no. 6, pp. 178–186, 2014, doi: 10.3151/jact.12.178.
- [7] F. U. A. Shaikh and S. W. M. Supit, "Mechanical and durability properties of high volume fly ash (HVFA) concrete containing calcium carbonate (CaCO<sub>3</sub>) nanoparticles," *Constr. Build. Mater.*, vol. 70, pp. 309–321, 2014, doi: 10.1016/j.conbuildmat.2014.07.099.
- [8] H.F.W.Taylor, *Cement Chemistry 2nd edition*. 1997.

	<b>Title</b> <b>Report on the assessment of the quality increase of cements enabled by the RECODE CO<sub>2</sub>- derived additives</b>	<b>Deliverable number</b> <b>D7.5</b>
		<b>Version</b> <b>Final</b>

- [9] J. M. Marangu, J. K. Thiong'O, and J. M. Wachira, "Review of Carbonation Resistance in Hydrated Cement Based Materials," *J. Chem.*, vol. 2019, 2019, doi: 10.1155/2019/8489671.
- [10] X. Liu, L. Chen, A. Liu, and X. Wang, "Effect of nano-CaCO<sub>3</sub> on properties of cement paste," *Energy Procedia*, vol. 16, no. PART B, pp. 991–996, 2012, doi: 10.1016/j.egypro.2012.01.158.
- [11] X. Liu, X. Wang, A. Liu, and L. Chen, "Study on the mechanical properties of cement modified by nanoparticles," *Appl. Mech. Mater.*, vol. 157–158, pp. 161–164, 2012, doi: 10.4028/www.scientific.net/AMM.157-158.161.
- [12] Y. Sun, P. Zhang, W. Guo, J. Bao, and C. Qu, "Effect of Nano-CaCO<sub>3</sub> on the Mechanical Properties and Durability of Concrete Incorporating Fly Ash," *Adv. Mater. Sci. Eng.*, vol. 2020, 2020, doi: 10.1155/2020/7365862.
- [13] J. Kawano, N. Shimobayashi, A. Miyake, and M. Kitamura, "Precipitation diagram of calcium carbonate polymorphs: Its construction and significance," *J. Phys. Condens. Matter*, vol. 21, no. 42, 2009, doi: 10.1088/0953-8984/21/42/425102.
- [14] J. D. Rodriguez-Blanco, S. Shaw, and L. G. Benning, "The kinetics and mechanisms of amorphous calcium carbonate (ACC) crystallization to calcite, via vaterite.," *Nanoscale*, vol. 3, no. 1, pp. 265–271, 2011, doi: 10.1039/c0nr00589d.
- [15] P.-C. Chen, C. Y. Tai, and K. C. Lee, "Morphology and growth rate of calcium carbonate crystals in a gas-liquid-solid reactive crystallizer," *Chem. Eng. Sci.*, vol. 52, no. 21–22, pp. 4171–4177, Nov. 1997, doi: 10.1016/S0009-2509(97)00259-5.
- [16] A. Declat, E. Reyes, and O. M. Suárez, "Calcium carbonate precipitation: A review of the carbonate crystallization process and applications in bioinspired composites," *Reviews on Advanced Materials Science*, vol. 44, no. 1. pp. 87–107, 2016.
- [17] European Standard EN 196-1, "European Standard EN 196-1, Methods of testing cement - Part 1: Determination of strength." 2016.
- [18] R. Gabrovšek, T. Vuk, and V. Kaučič, "Evaluation of the hydration of Portland cement containing various carbonates by means of thermal analysis," *Acta Chim. Slov.*, vol. 53, no. 2, pp. 159–165, 2006.
- [19] X. Ouyang, Z. Pan, Z. Qian, Y. Ma, G. Ye, and K. van Breugel, "Numerical modelling of the effect of filler/matrix interfacial strength on the fracture of cementitious composites," *Materials (Basel)*, vol. 11, no. 8, 2018, doi: 10.3390/ma11081362.
- [20] C. W. Hargis, A. Telesca, and P. J. M. Monteiro, "Calcium sulfoaluminate (Ye'elimite) hydration in the presence of gypsum, calcite, and vaterite," *Cem. Concr. Res.*, vol. 65, pp. 15–20, 2014, doi: 10.1016/j.cemconres.2014.07.004.
- [21] Ente Nazionale Italiano di Unificazione (UNI), "Testing Fresh Concrete—Part 2: Slump Test; UNI EN 12350-2:2019." Milan, Italy, 2019.
- [22] Ente Nazionale Italiano di Unificazione (UNI), "Testing Fresh Concrete-Part 6: Density; UNI EN 12350-6:2019." Milan, Italy, 2019.

	<b>Title</b> <b>Report on the assessment of the quality increase of cements enabled by the RECODE CO<sub>2</sub>-derived additives</b>	<b>Deliverable number</b> <b>D7.5</b>
		<b>Version</b> <b>Final</b>

- [23] Ente Nazionale Italiano di Unificazione (UNI), “Testing Hardened Concrete—Part 3: Compressive Strength of Test Specimens; UNI EN 12390-3: 2019.” Milan, Italy, 2019.
- [24] Ente Nazionale Italiano di Unificazione (UNI), “Testing Hardened Concrete-Part 8: Depth of Penetration of Water Under Pressure; UNI EN 12390-8: 2009.” Milan, Italy, 2009.
- [25] A. Fehervari, A. Macleod, E. O. Garcez, and W. P. Gates, “RHEOLOGICAL BEHAVIOUR OF CONCRETE ENRICHED WITH CARBON RHEOLOGICAL BEHAVIOUR OF CONCRETE ENRICHED WITH CARBON NANOFILLERS,” no. September, 2018.
- [26] S. Chandra, A. S. Van Rooyen, G. P. A. G. Van Zijl, and F. L. Petrik, “Properties of cement-based composites using nanoparticles: A comprehensive review,” *Constr. Build. Mater.*, vol. 189, pp. 1019–1034, 2018, doi: 10.1016/j.conbuildmat.2018.09.062.
- [27] S. Khalilpour, E. Baniasad, and M. Dehestani, “A review on concrete fracture energy and effective parameters,” *Cem. Concr. Res.*, vol. 120, pp. 294–321, 2019, doi: 10.1016/j.cemconres.2019.03.013.